Biochimica et Biophysica Acta, 688 (1982) 673–684
Elsevier Biomedical Press

BBA 71180

THE DEPENDENCE OF THE CONDUCTANCE OF THE HEMOCYANIN CHANNEL ON APPLIED POTENTIAL AND IONIC CONCENTRATION WITH MONO- AND DIVALENT CATIONS

G. MENESTRINA and R. ANTOLINI

Dipartimento di Fisica, Libera Università degli Studi, I 38050 Povo (TN) (Italy)

(Received October 26th, 1981)
(Revised manuscript received February 1st, 1982)

Key words: Conductance; Hemocyanin channel; Voltage gating; Black lipid membrane; Potential difference; Ion concentration

Incorporation of *Megatura crenulata* hemocyanin into phosphatidylcholine black lipid membranes results in the formation of ion channels. Channel properties depend on many factors, three of which are examined in this work: type and concentration of electrolyte and applied voltage. Eight cations at different concentrations have been used. Instantaneous conductance of the channel is a saturating function of both applied voltage and ionic strength of the bathing solution with monovalent cations, but only of ionic strength with divalent cations. Steady-state voltage-conductance relations are nonlinear for both signs but show slight saturation with ionic strength. Relaxation towards the steady state can be fitted by two exponentials with different time constants. All experimental data are fitted postulating the existence of a mechanism of voltage gating of the channel, and of discrete negative charge near its mouth. Specific and nonspecific binding of cations is required.

Introduction

Hemocyanins are respiratory copper proteins of large molecular weight which occur freely dissolved in the hemolymph of a number of invertebrates [1]. In 1972 it was first demonstrated that one of these, extracted from the blood of the giant keyhole limpet *Megatura crenulata*, interacts with black lipid membranes, forming ion channels [2]. Now it seems that molluscan hemocyanins are a general class of pore-forming substances [3,4]. The *M. crenulata* hemocyanin channel has several possible conductance states and transitions between these different levels are voltage dependent. The conductance of each level is a nonlinear function of applied potential, and that of the first level is also a nonlinear function of the concentration of the electrolytic solution [5].

A previous study, performed on oxidized cholesterol membranes with the chlorides of four cations (Na^+, K^+, Ca^{2+}, Ba^{2+}) demonstrated that the properties of the channel are determined for the most part by a negative charge fixed to it. This was confirmed by the pH dependence of the channel conductance [6]. In this study we have undertaken a more systematic study of the dependence of channel conductance on both the applied potential and the ionic strength with the chlorides of eight cations (Li^+, Na^+, K^+, Cs^+, Mg^{2+}, Ca^{2+}, Sr^{2+}, Ba^{2+}) using phosphatidylcholine black lipid membrane.

The nonlinearity of the variation of conductance with voltage is explained by postulating the existence of a gating mechanism, while the nonlinearity with concentration is explained by assuming that the channel is negatively charged. A discrete

Abbreviation: Bistris, 2-(bis(2-hydroxyethyl)amino)-2-(hydroxymethyl)-1,3-propanediol.

0005-2736/82/0000–0000/$02.75

charge theory, instead of a smeared charge one such as that of Guy-Chapman as used in Ref. 6, is adopted in our new model.

The existence of a binding site for divalent cations is necessary to explain all of our results. The binding of divalent cations to free hemocyanin is well known [1], and the binding of these ions to the hemocyanin channel has been reported recently by us [7]. Little is known about the structure of the channel. Hemocyanin molecules in solution at pH 7.0 are hollow cylinders with both length and external diameter of about 30 nm [1], but the channel may be due to a different state of aggregation of the subunits. An electron microscopic approach to the problem has been tried by McIntosh et al. [8]. They reported that a possible channel-forming structure is an annulus about 7 nm in diameter, which protrudes into the solution for about 3 nm and contains a central pool of staining which is 2 nm in diameter, and may be related to the ionic pathway.

Materials and Methods

Black lipid membranes are obtained by the usual technique [9] using saturated phosphatidylcholine from egg lecithin purchased by P.L. Biochemicals. The product is more than 99% pure, gives one spot by TLC, and is diluted in *n*-decane to a final concentration of 50 mg/ml.

The Teflon sept separating the two compartments has a circular hole of about 0.5 mm diameter. Electrolytic solutions are prepared using Carlo Erba RPE salts and are buffered by 10 mM Bistris (Calbiochem) when salt concentration is more than 100 mM, and by 10% Bistris when it is less. The pH is adjusted to 7.0 with HCl. The specific conductance of the solution is measured at 4 kHz with a conductivity cell whose cell constant is 2 cm^{-1}. *Megatura crenulata* hemocyanin, A grade in 50% glycerol, is purchased from Calbiochem and stored at −20°C. Small amounts of a 2 mg/ml stock solution are added to the solution in contact with one side of the black lipid membrane when this membrane is completely formed. This procedure ensures complete orientation of the channels [10]. Electrical signals are taken through Ag-AgCl electrodes; and the current is amplified by a virtual grounded operational amplifier (AD 515 K) with a parallel circuit of $10^8\,\Omega$, 20 pF or $10^7\,\Omega$, 200 pF in the feed-back loop. In this configuration the potential across the membrane is essentially equal to the source potential and voltage clamp conditions are attained without an external feed-back. Amplified current and voltage signals are monitored on a Tektronix 7613/ 7A22 and 7A18 storage oscilloscope, and recorded on a chart recorder. The protein containing compartment is taken as the reference for voltage sign. All of the experiments were performed at room temperature, which ranged from 20 to 23°C.

The following stimulating procedures have been adopted in measurements on many channels in order to make the required corrections for the continuous, slow incorporation of hemocyanin molecules:

(a) Instantaneous current vs. voltage curves. A short train of positive and negative pulses, typically three of each sign, of equal amplitude is applied. Then the amplitude is increased by 10 mV. New trains are applied till a maximum amplitude of around 120 mV is reached, then the amplitude is decreased, again in steps of 10 mV, till it reaches zero. Between one short train and the other the membrane is grounded for some seconds. The result of this stimulation is the pattern of current steps shown in Fig. 2a. Corrections have been made assuming a linear increase in conductance between the first and the second short train of pulses of the same voltage and by then extrapolating all measured values of current to the values that would be found at a particular time. Incidentally using this technique we have also seen that the rate of incorporation of channels into the black lipid membrane is independent of the applied voltage. In fact the straight line that can be extrapolated between the three pulses of the first short train always fits also the pulses of the second train, irrespectively of differences in the pulse protocol between the first and the second train.

(b) Steady-state current vs. voltage curves. Long-lasting pulses of different values and signs were applied till a maximum amplitude of ±120 mV. The holding potential between the pulses was chosen in order to open all of the channels quickly. The results are shown in Figs. 5, 6, 7 part a. Gradual increases of conductance were detected by application of ±10 mV pulses in the course of

the experiment and corrections were made by a linear extrapolation through the measured amplitude of the current. Moreover, in order to distinguish between the nonlinearity intrinsic to each conductance level of the channel [5] and that arising from voltage-dependent transitions between different levels, each point was normalized by dividing by the instantaneous conductance value. In this way we obtain the steady-state conductance as a fraction of the conductance of the first level.

Results

Channel formation

Addition of small amounts of *M. crenulata* hemocyanin to the solution in contact with a black lipid membrane, yields a stepwise increase of current, each step being due to the formation of an ion channel through the lipid bilayer [5]. Under voltage clamp conditions the magnitudes of these steps show a reproducible distribution around a mean value [6]. This value has been taken as the conductance of the channel in its first conductance level under a fixed set of experimental parameters, i.e. applied voltage, type and concentration of salt, temperature and lipid composition of the black lipid membrane (Fig. 1, a). Formation of channels is virtually irreversible and this produces a continuous gradual increase of current of up to many orders of magnitude [2]. The rate of this increase is strongly dependent on the concentration of the protein in solution [11]. At the hemocyanin concentrations used in our experiments (10–100 μg/ml), roughly a thousand channels are present in the membrane after one hour, and the continuous current increase at constant applied voltage may be considered to a good approximation to be small and linear (Fig. 1, b). All current-voltage measurements described in the next two sections were carried out under these conditions.

Instantaneous current-voltage curves

Once the membrane contains sufficient channels to exhibit a linearly increasing conductivity a series of voltage pulses are applied. Each pulse lasts about 500 ms, a time long enough to allow current registration on the *X-t* recorder, but short enough to prevent channel relaxation towards

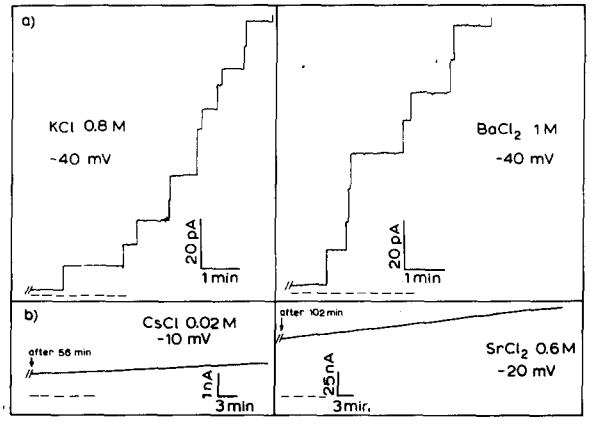

Fig. 1. (a) Current steps observed after the addition of 10^{-5} g/ml of hemocyanin to a phosphatidylcholine/*n*-decane black lipid membrane. Each jump is due to the opening of a new channel through the membrane. (b) Linear current increase due to continuous incorporation of hemocyanin molecules into the lipid film, after about one hour from the addition of the protein. Note that time scale is longer than in (a). Left: monovalent cations; right: divalent cations.

lower levels of conductance (Typical time constants of this relaxation are many seconds [5] as will be shown in the next section). The response is a series of current pulses. In comparing the magnitudes of the current pulses obtained at different voltages one must take into account that differences in current arise not only from the change in potential but also from the change in the number of channels present in the membrane as a function of time. Corrections for the latter effect were performed following the procedure described in Methods and shown in Fig. 2.

Repeated application of this procedure leads to plots of current as a function of voltage that are superimposable after a simple normalization for the differences in the number of channels present. This means that the channels are independent of each other. Earlier studies [5,12] have already shown that the properties of a single channel are in complete agreement with the properties of membranes containing many channels. Thus, the current-voltage curves we obtain after normalization represent the properties of the single channel in its first conductance level, transition towards lower levels being excluded by the short duration of the voltage pulses. A set of experiments has

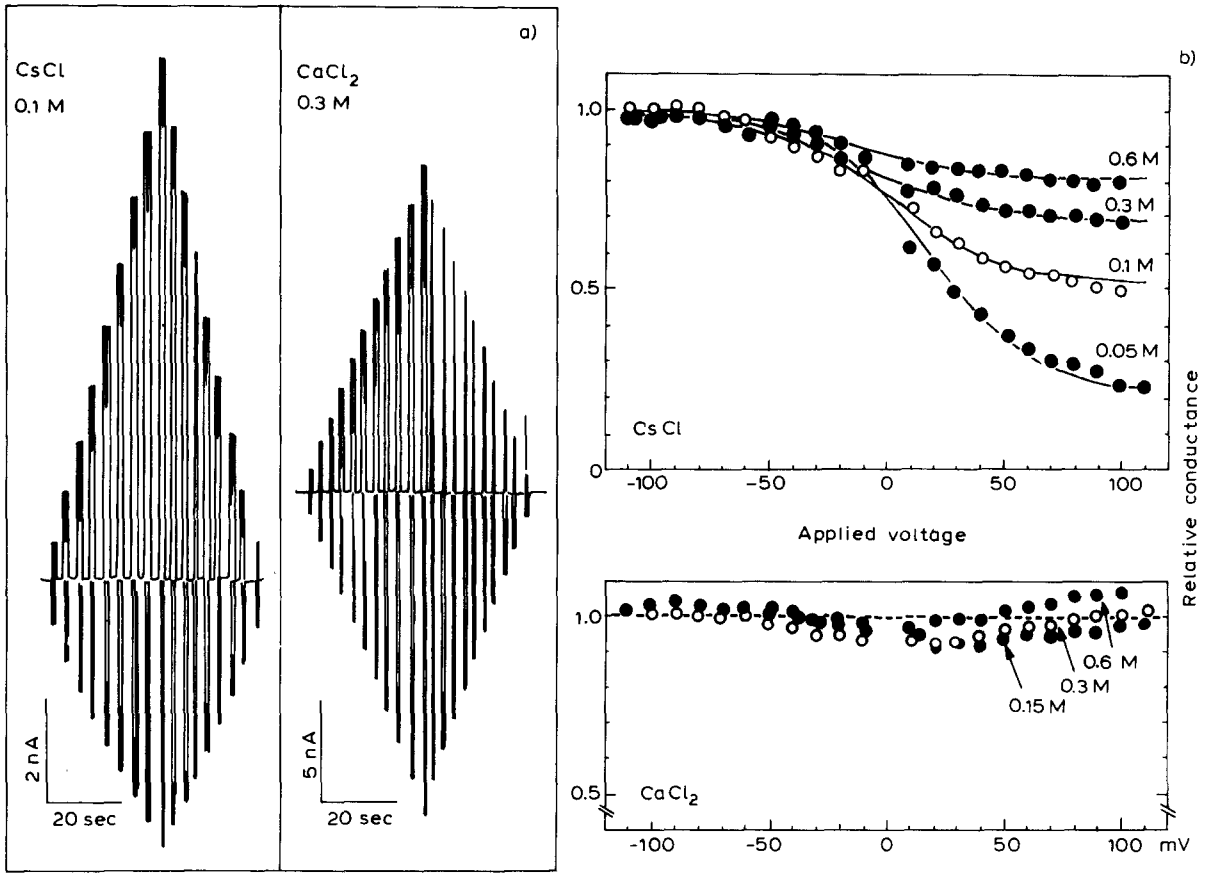

Fig. 2. (a) Instantaneous current-voltage curves obtained adopting the stimulation procedure described in Materials. They may be linear or not depending on electrolyte conditions. The nonlinearity increases when cation concentration is decreased as shown in part (b). (b) Relative channel conductance vs. voltage, obtained dividing by the maximum conductance of the system. Upper part: S-shaped curves obtained with one monovalent cation, solid lines are best fit to the points using Eqn. A1. Lower part: with divalent cations the conductance is practically constant; dashed line drawn by hand. Open circles are taken from the patterns of part (A).

been performed with electrolytic solutions containing only one salt at a time. The chlorides of four metals of the first group and four of the second group have been used in different concentrations. Instantaneous current-voltage curves are always nonlinear when monovalent cations are used, while they are practically linear in the presence of divalent cations. This can be seen more clearly if the experimental data are used to compute conductance as a function of voltage. Such plots are S-shaped when monovalent cations are used, conductance being lower for positive potentials, while the voltage dependence disappears when divalent cations are used. The S-shaped curves typical of monovalent cations are very sensitive to both the type and the concentration of the cation. As a general rule the nonlinearity increases when the cation radius increases, and when its concentration decreases. Experimental points are fitted to Eqn. A1. From these fits we obtain both the maximum and the minimum conductance of the open channel as a function of the type and concentration of the electrolyte (see Appendix A).

Experimental points for monovalent cations are presented in Fig. 3. One can see that both the high and the low values of conductance are nonlinear functions of ionic concentration, showing a saturation effect. Saturation of the high channel conductance was observed also in oxidized cholesterol membranes and attributed to a fixed negative

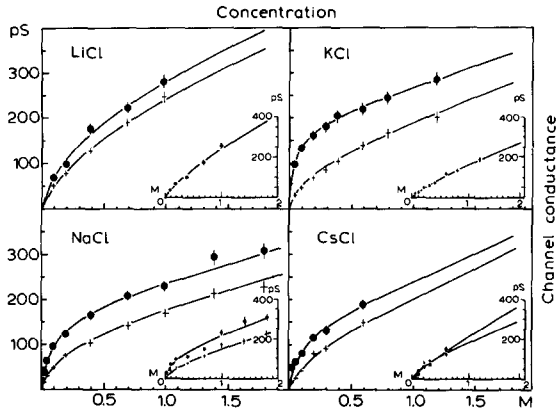

Fig. 3. Conductance vs. concentration with four monovalent cations. Full circles represent the high conductance value, $G(A)$, of the channel in the first level; simple crosses the low value, $G(B)$. The insets are the steady-state values of conductance for high negative potentials, full circles, and for high positive potentials, simple crosses. Solid lines are drawn using Eqns. A2 and A3 with the values listed in Table I; conductance and concentration scales are the same for all the graphs.

charge on the pore [6]. This effect is less pronounced in the low-conductance curves suggesting a smaller amount of fixed charge. With divalent cations the same saturating behaviour is observed (Fig. 4) but no difference is seen between high and low conductance. Therefore we present only one curve for each of these cations.

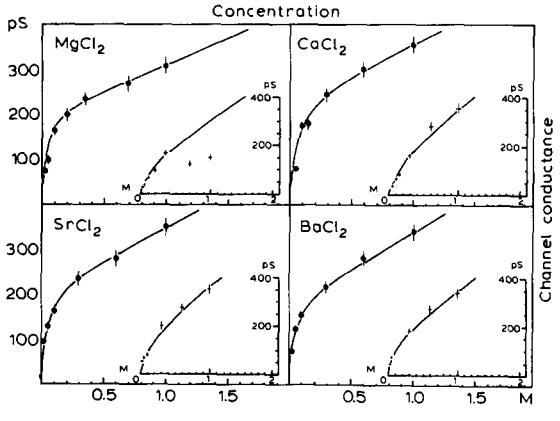

Fig. 4. Conductance vs. concentration with four divalent cations. Full circles represent the instantaneous conductance of the channel, $G(A)$; while simple crosses in the insets are the steady state conductance at high negative voltages. The strong deviation of $MgCl_2$ at high concentration is due to on-off fluctuations observed only with this salt, which are not accounted for by the model. Scales and solid lines are as in Fig. 3.

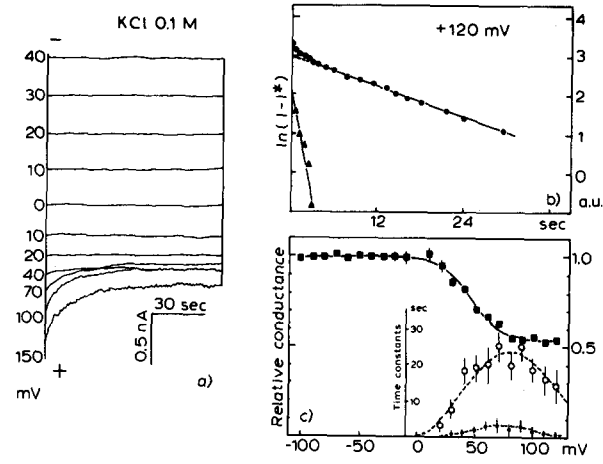

Fig. 5. (a) Current relaxations after the application of long-lasting voltage pulses of the indicated value, to an hemocyanin doped black lipid membrane bathed by 0.1 M KCl. The procedure is described in Materials. Current increases linearly with applied negative potentials, but relaxes to lower steady-state values with positive potentials. (b) Circles: half logarithmic plot of the relaxation amplitude $I - I^*$, where I^* is the steady-state current. A first-order relaxation may be extrapolated only from a certain point; triangles: fast relaxation alone, after subtraction of the slow one. (c) Full squares: relative conductance of the channel in the steady-state condition, expressed as a fraction of the conductance of the first level, vs. applied voltage. Solid line is a best fit with Eqn. A1. Full and open circles are the two time constants shown in part (b) as a function of applied potential. Vertical bars arise from differences in repeated measurements. Dashed lines drawn by hand.

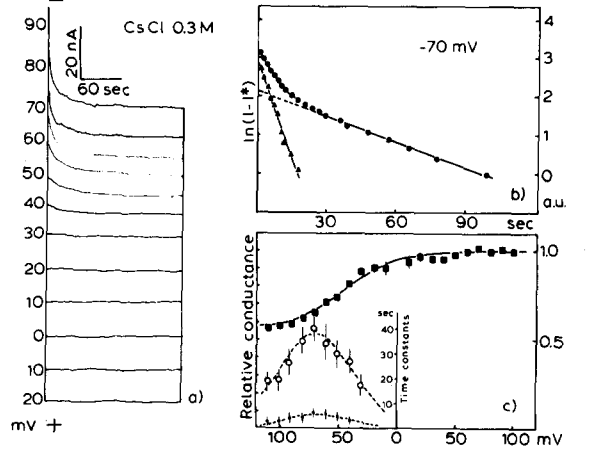

Fig. 6. Same parameters as in Fig. 5, but the solution contains 0.3 M CsCl. The conductance-voltage curve is reversed and relaxation towards lower levels occurs for applied negative voltages.

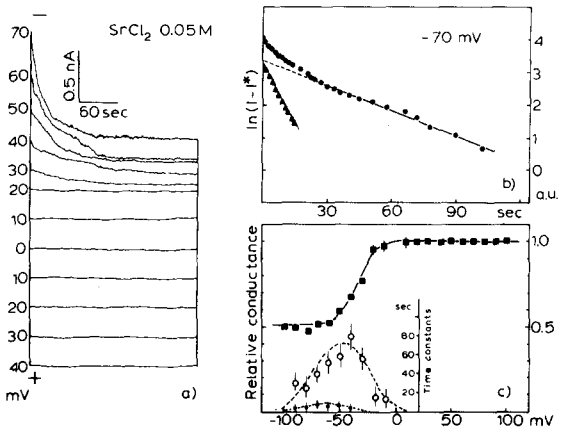

Fig. 7. Same parameters as in Fig. 5, but a divalent cation is used. With divalent cations only the negative steady-state nonlinearity has been observed. Note that the time constants are always in the range of several seconds.

Steady-state current-voltage curves

With membranes containing sufficient channels to exhibit a slow linear increase of conductance with time we apply a series of pulses of different voltage, according to the pulse procedure described in Methods. Each pulse lasts long enough, usually some minutes, to allow complete relaxation of the system towards the new steady state. In this way we can observe current relaxations towards lower conductance levels both for positive and negative potentials depending on the cation present in the solution. The nonlinearity observed with negative applied voltages has never been described before but is common to all the cations with the exception of K^+. With two cations, Na^+ and Cs^+, the channel exhibits a transition to lower conductance for both positive and negative potentials. Current relaxations following step

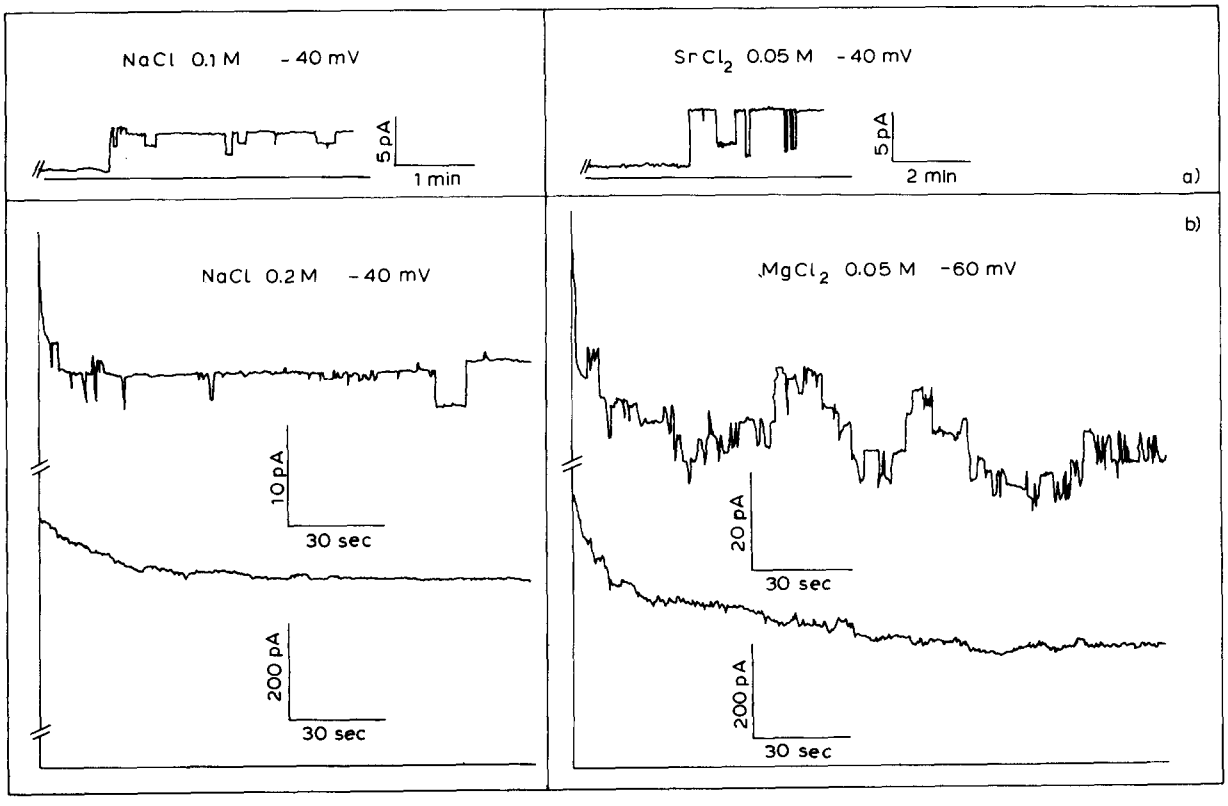

Fig. 8. (a) Current steps due to the formation of one hemocyanin channel followed by fluctuations between different conductance levels. (b) Current relaxations after potential jumps in membranes containing few (upper traces) and many (lower traces) hemocyanin channels. Different current scales, but equal time scales are used. Discrete conductance fluctuations are evident with few channels. Left: monovalent cations; right: divalent cations.

changes of voltage are presented in part a of Figs. 5–7 for three different cations. The relaxation is not a simple exponential as can be seen in part b of these figures where semilogarithmic plots of the current transient are shown. At least two exponentials are needed to fit the experimental points, the second being calculated after subtraction of the first. The two time constants are similar functions of the applied voltage showing a pronounced maximum, while the steady-state conductance-voltage curve is S-shaped, typical of excitability. The conductance and the two time constants are shown as a function of applied voltage in part c of Figs. 5–7.

Repeated measurements on the same membrane gave identical time constants while the observed conductances were superimposable after suitable normalization.

From single channel experiments it is evident that the channel possesses different conductance levels and can fluctuate between them. Two examples are shown in Fig. 8a. Current traces of Fig. 8b, obtained with membranes containing few channels, show that relaxation after a potential jump arises from transitions of all the pores through these levels. The comparison with traces from a membrane containing many channels in Fig. 8c shows that the time constants do not depend on the total number of pores present. As in the case of instantaneous conductance-voltage curves, the S-shaped steady-state conductance curves are dependent on ionic strength. Once again increasing ion concentration decreases the nonlinearity of the curve. We are unable to say if there is an effect of ionic strength on the observed time constants, due to an insufficient reproducibility of these data in different membranes.

Discussion

A model for the first level of the channel

Instantaneous conductance-voltage curves representing the channel in the first level of conductance, obtained with monovalent cations, exhibit a characteristic sigmoid shape. This reminds us of other excitable channels, such as EIM*, and on this basis we can interpret this nonlinearity by making use of a simple gating model that has already been described elsewhere [13,14]. A different model which assumes only that the channel is asymmetrically charged is also discussed at the end of this subsection.

We assume that the channel in the first level can fluctuate between two conformations, say A and B, with different conductances, $G(A)$ and $G(B)$. These fluctuations should have time constants of less than milliseconds and would therefore not be resolved by our experimental set-up. Transition between the two configurations, which are separated by a conformational energy barrier, is promoted by the movement of a charged group that, we suppose, experience all the applied voltage. In this case, the conductance of the channel, $G(V)$, is given by Eqn. A1 (see Appendix A) and varies between $G(A)$ and $G(B)$ with an S-shaped dependence on voltage.

All our experimental curves, more than 50, which were obtained at different concentrations of the chlorides of Li^+, Na^+, K^+ and Cs^+ have been fitted to Eqn. A1 allowing all of the parameters to vary independently. Although the curves are very different in shape, they all yield the same gating charge whose average value is 1.1 ± 0.2 elementary charges. The two conductance values $G(A)$ and $G(B)$ can be calculated separately for each monovalent cation and plotted as a function of concentration to give the saturating curves of Fig. 3. When only divalent cations are present no S-shaped curve is seen, implying that in this case $G(A) = G(B)$ and both are equal to the conductance measured by the incorporation jumps. Saturation observed in Fig. 3 can be explained by assuming that the pore bears some fixed point charges. In this case the conductance of the channel is proportional to the concentration of ions at its mouth and not to that in the bulk solution. Based on this we have to calculate the potential generated by the discrete charges and then to use it to determine the local ion concentrations. This is done in Eqns. A2, A3 of appendix A.

All of our experimental curves, shown in Figs. 3 and 4, have been fitted in this way by making use of the literature values for the mobilities of cations in free solution. The parameters used are listed in Table I. From Table I we can see that the geometrical factor is practically a constant whose value is

* EIM, excitability inducing material.

TABLE I

PARAMETERS USED IN EQNS. A2 AND A3 TO FIT EXPERIMENTAL POINTS OF FIGS. 3 AND 4

The parameter of the first column is a geometrical factor ($\pi r^2/l$) which takes into account the dimensions of the pore. If we consider that the mobility of the ion in the pore, ω_p, may be different from that in free solution, ω_{sol}, that we have used, we must say that the parameter is rather $(\pi r^2/l)\cdot(\omega_p/\omega_{sol})$. The parameters of the other columns derive from the use of the Nelson-McQuarrie potential and are: $4Z$, total fixed charge per pore in electromagnetic units (e.u.); d, half-distance between discrete charges on the pore; a and a', spacing of charged lipids and pores, respectively. For all experiments $a = 10$ nm and $a' = 50$ nm. For each cation the different rows indicate different states of the channel, that is: A and B, two possible conformations of the first level; SS^+ and SS^-, steady-state conformations for positive and negative voltages, respectively. n.o., not observed.

		$\pi r^2/l$ (pm)	$4Z$ (e.u.)	d (nm)
CsCl	A	6.5	1.12	0.37
	B	6.5	0.76	0.37
	SS^+	8.0	0.36	0.37
	SS^-	6.0	0.72	0.37
KCl	A	6	1.32	0.31
	B	5.8	0.80	0.31
	SS^+	6.1	0.48	0.31
	SS^-	n.o.		
NaCl	A	7	0.98	0.29
	B	6.5	0.76	0.29
	SS^+	6.9	0.52	0.29
	SS^-	8.2	0.72	0.29
LiCl	A	12	0.52	0.23
	B	12	0.42	0.23
	SS^+	n.o.		
	SS^-	15	0.28	0.23
$BaCl_2$	A	6.0	0.48	0.23
	SS^-	7.2	0.32	0.23
$SrCl_2$	A	5.8	0.44	0.21
	SS^-	7.7	0.26	0.21
$CaCl_2$	A	5.3	0.40	0.23
	SS^-	7.5	0.20	0.23
$MgCl_2$	A	5.5	0.48	0.25
	SS^-	7.3	0.26	0.25

$(6.0 \pm 0.5)\cdot 10^{-3}$ nm. This means that the mobilities of the cations in the pore are proportional to those in free solution, implying that the channel is hydrated. The only exception is Li^+, which has a geometrical factor of $(12 \pm 1)\cdot 10^{-3}$ nm, which implies a mobility in the pore which is twice that of the other cations. A possible explanation could be the presence of a highly organized form of water inside the channel. There is in fact theoretical evidence suggesting that in this case the mobility of small cations will be strongly enhanced [15].

The diameter of the channel entrance can be estimated from the parameter d and seems to be sensitive to the cation species being used, ranging from 0.6 nm for Ca^{2+} to 1 nm for Cs^+. However this deduction is not strictly correct as is discussed in Appendix A.

The total charge on the channel depends strongly on the cation present in solution. It is maximum for K^+, decreases for Cs^+ and Na^+, and is minimum for Li^+ and the divalent cations. Besides this the two conformations A and B bear different charges, that of state B always being smaller. This means that the transition between the two states, induced by the movement of the gating charge, has the effect of diminishing the total charge on the channel thus influencing the conductance pathway. This could occur for example by infolding the charge into the protein. The charge difference between state A and B is again maximum for K^+, smaller for Na^+ and Cs^+, minimum for Li^+ and null for all divalent cations. This can be explained by assuming that a part of the total charge of the channel, involved in the transition from A to B, resides in a negative site which can bind divalent cations and also small monovalent cations such as Li^+. It is worth noting that the binding of divalent cations by hemocyanin is well known [1], and it has been hypothesized that hydrogen ions can also bind to these same sites [16]. Dissociation constant for Ca^{2+} have been estimated to be 13 mM.

Binding of divalent cations to the hemocyanin channel has recently been demonstrated by us [7], by studying their ability to diminish the conductance of the channel 0.1 M KCl when added in mM concentrations. Dissociation constants were estimated to be 5 and 10 mM for Ca^{2+} and Ba^{2+}, respectively. Transition from state A to B could be accompanied by the movement of this site so that it is no longer at the entrance of the pore. On the other hand at our cation concentrations the site

would be always occupied, and hence neutralized, when divalent cations are used, thus reducing the total charge of the channel to a minimum and eliminating completely the difference in charge and in conductance between state A and B. In this picture, Li^+ can also bind to the same site but doesn't completely neutralize it because of its univalent charge.

Now we want to discuss briefly an alternate explanation for the S-shaped conductance-voltage curves we have obtained, based on a different model. If the conductance properties of the channel arise from a negative fixed charge which creates a strong potential at its mouth, we may suggest that the two mouthes of the pore are differently charged. In this case we would have different cation concentrations at the two entrances of the pore and this would produce the effect that an electric field applied from the side of higher concentration towards the other will generate more current than an electric field in the opposite direction. This effect has been observed and described with hybrid channels obtained by dimerization of Gramicidin A and *O*-pyromellitylgramicidin, a negatively charged derivative of Gramicidin [17,18]. Furthermore an increase in the ion concentration would lead to a decrease of the nonlinearity due to the screening of the fixed charges, as we have observed. The solution of the Nernst-Plank equation in this case, see Appendix B, leads to an expression for $G(V)$ that has the required S-shape varying between the same asymptotic values of Eqn. A2. The discussion of the saturating properties would be the same as above, the only difference being that now A and B are not different conformations but only the two differently charged mouthes of the channel. This model has the advantage of describing both saturation phenomena, that at high concentrations and that at high applied voltage, merely by assuming that the channel is asymmetrically charged. Unfortunately Eqn. B4 though being S-shaped, cannot fit our data because it requires a larger voltage interval to reach the asymptotic values, about 400 mV against 100 mV of our curves. However, this may be due to the approximations we have used to obtain this relationship.

Fluctuations between different levels of the channel

The *M. crenulata* hemocyanin channel possesses many conductance levels. At least four can be distinguished in 0.1 M KCl [5,19]. Transitions between these levels are strongly dependent on voltage and we have now presented evidence that they are also dependent on type and concentration of the electrolyte.

Steady-state conductance is determined by transitions between the different levels and is generally S-shaped. When large monovalent cations are used transitions to lower levels of conductance occur for positive potentials, while for example when divalent cations are used lower conductance is obtained by applying negative potentials.

This allows us to state that there are two regions of nonlinearity in the steady-state conductance-voltage curve, as occurs for example with EIM [20], one for positive and one for negative potentials. Both regions are present under some conditions but one may be absent depending on ionic species present in the solution. Current relaxation after a step in potential, both for positive and negative voltages, are not simple exponentials, and this is of course the result of multiple relaxations through the different conductance levels. In any case each current transient may be fitted reasonably well by two simple exponentials with different constants of time, implying a minimum of three distinct levels. By analogy with the two-state case [13], one would expect that time constants are a function only of the final and not of the starting potential. This has been verified quantitatively only in the case of 0.1 M KCl [19], but seems to us to hold true in all the measurements reported here. The time constants should be 'bell-shaped' functions of the final potentials, being null for large positive and negative voltages and coming to a maximum near to the middle of the S-shaped conductance-voltage curve, and this has been verified in our experiments. S-shaped curves have been fitted making use of Eqn. A1, A and B representing in this case the first and the last level of the channel. However in this case the gating charge is found to be a constant, but ranges from 2 to 4 elementary charges. This we think, is due to the fact that different transitions, between differ-

ent levels, are averaged in the S-shaped curve by varying the electrolyte.

The following empirical rule to predict whether poisitive or negative nonlinearity regions will be found, seems to hold: if the total charge of the channel as given in Table I is more than that of Li^+, the positive region is found. If the total charge of the channel is less than that of K^+ the negative region will be found. One can see that there is an overlap between the two regions, and in fact Na^+ and Cs^+ show both regions of nonlinearity. A possible interpretation of this sequence is that there are two energy minima for the gating charges that produce the transition between the conductance levels. One is reached by applying positive voltages and one by applying negative voltages. These two minima are greatly influenced by the total charge of the channel, that is by the state of the negative site discussed in the previous section. When the site is free the positive minimum is favoured while when the site is occupied by Li^+ or one divalent cation the negative minimum is strongly favoured. This model can explain the fact that both Li^+ and divalent cations reduce the conductance of the channel to 0.1 M KCl, in the negative region, when added in mM [6,20]. Under these conditions the site is progressively titrated, and the effects are transitions to lower levels of conductance. Incidentally this is also the reason for a previously reported anomalously low conductance of the channel in 0.1 M LiCl when negative potentials are applied [21].

We have observed that for a given cation the non linearity of the S-shaped conductance curves decreases as the ionic strength is increased, as is the case for the instantaneous conductance-voltage curves. This may be due either to the fact that certain low conductance levels become unfavourable as the number of positive ions in the channel increases, or to the fact that the difference in conductance between the first and the last level is a decreasing function of the ionic strength. Discrimination between the two models would only be possible by single channel measurements and will be the subject of future work. Following the second idea we may think that the difference in conductance between the first and the last level is due, also in this case, to a different charge of the channel. So, making use of Eqns. A2 and A3 we may fit our data. The results are shown in the insets of Figs. 3 and 4 and the parameters used are listed in Table I. We can see that the movement of the gating charges is accompanied by a decrease of the charge influencing the conducting pathway and by a slight increase of mobility of cations in the channel.

Since the preparation of this paper some new data have been presented by Cecchi et al. [26] which confirm our results. Instantaneous current-voltage curves of membranes containing many hemocyanin channels have been shown to depend on ionic concentration of Li^+ and K^+ in a way similar to our findings. Data have been explained by these authors with a single file model which calls for three energy barrriers in the channel, a total of seven free parameters had to be used.

Appendix A

A simple two-state gating model, as described for example in Ref. 13 predicts that the conductance of the channel $G(V)$ is given by:

$$G(V) = G(B) + (G(A) - G(B))/(1 + \exp(q(V - V_0)/kT)) \quad (A1)$$

where $G(A)$ and $G(B)$ are the channel conductances in state A and B. The states are attained with large negative and large positive potentials, respectively. q is the gating charge; V is the applied potential. qV_0 is the conformational energy change between the two configurations.

Data from membranes with many channels were first best fitted with Eqn. A1, and then normalized by dividing by the higher asymptote to give a relative conductance as shown in Fig. 2. Single-channel conductance is then obtained by multiplying by the factor which gives the absolute current value that was measured at a fixed voltage, usually -40 mV, during the initial incorporation of hemocyanin.

To calculate the contribution of each ion species to the conductance of the channel we suppose now that this is a cylindrical pore filled with water, with a fixed charge on it, determining a local

concentration of ions different from that in the bulk. We have then:

$$G(\alpha) = (\pi r^2/l) z e_0 \omega_p C_0 \exp(-z e_0 \psi(\alpha)/kT) \quad \text{(A2)}$$

where: α may be A or B; r and l are radius and length of the pore, respectively; z, C_0 and ω_p are valence, concentration in the bulk and conventional mobility in the pore of the ion, respectively; e_0 is the elementary charge; k and T have their usual meaning; and $\psi(\alpha)$ is the potential created at the entrance of the pore by the distribution of fixed charges.

From Eqn. A2 one can see that if $\psi(\alpha)$ is great enough only counter ions contribute substantially to the conductance of the pore, thus to explain cation selectivity of the channel [21,22] we have to assume that it is negatively charged. The potential $\psi(\alpha)$ in the case of discrete negative charges fixed on the pore, may be calculated following the procedure indicated by Nelson and McQuarrie [23]. They discussed a model in which both a square lattice of elementary charges with spacing a, representing the charged lipids of the membrane, and a square lattice of equal, charged pores with spacing a' are considered. Each channel is thought to bear four equal point charges of valence Z located in square shape on a circle of radius r. Combining Eqns. 32 and 35 of Ref. 23 we obtain:

$$\psi(\alpha) = \frac{e_0}{2\pi\epsilon}\left\{\frac{1}{a}\sum_{h,k}\frac{\exp\left\{\kappa a\left[\left(\frac{1}{2}-h\right)^2+\left(\frac{1}{2}-k\right)^2\right]^{1/2}\right\}}{\left[\left(\frac{1}{2}-h\right)^2+\left(\frac{1}{2}-k\right)^2\right]^{1/2}}\right.$$

$$\left. + \frac{Z(\alpha)}{a'}\sum_{m,n}\frac{\exp\left\{-\kappa a'\left[\left(\pm\frac{d}{a'}-m\right)^2+\left(\pm\frac{d}{a'}-n\right)^2\right]^{1/2}\right\}}{\left[\left(\pm\frac{d}{a'}-m\right)^2+\left(\pm\frac{d}{a'}-n\right)^2\right]^{1/2}}\right\} \quad \text{(A3)}$$

Where the notation '$\pm$' denotes a summation over the four possible combination $+(d/a')-m$ and $+(d/a')-n$, $+(d/a')-m$ and $-(d/a')-n$, etc. and κ = Debye-Hückel coefficient; ϵ = dielectric constant of water; h, k, m, n = integers ranging from 0 to ∞; d = half-distance between the fixed charges of the pore, that is $d = r/\sqrt{2}$; all the other symbols are as previously defined.

Obviously the potential is a function of the total charge of the system, but also of the type and concentration of ions in solution through the Debye-Hückel coefficient, due to screening of the fixed point charges. From Eqn. A3 we were able to evaluate numerically the potential and then substitute this value into Eqn. A2 to fit the experimental points of Figs. 3 and 4.

The use of the dielectric constant of free water in Eqn. A3 may be a questionable approximation since we have no information about the state of water at the mouth of the pore. However Eqn. A3 is in fact somewhat redundant; taking into account the very high values of a and a' used Eqn. A3 can be reduced to the form

$$\psi(\alpha) = \frac{4Z(\alpha)e_0}{2\pi\epsilon}\frac{\exp(-\kappa\sqrt{2d})}{\sqrt{2d}} \quad \text{(A4)}$$

which may be rewritten, putting $Q(\alpha) = 8Z(\alpha)e_0$, to give

$$\psi(\alpha) = \frac{Q(\alpha)}{4\pi\epsilon}\frac{\exp(-\kappa r)}{r} \quad \text{(A5)}$$

This is the potential created in solution by a single point charge $Q(\alpha)$ at a distance r [24].

For this reason we cannot interpret r as a real measure of the radius of the pore, as in the Nelson model, but rather as an upper limit of the true value.

Appendix B

A complete resolution of the Nernst-Planck equation in the case of an asymmetrically charged membrane separating two acqueous solutions can be found in [25]. In our case this leads to the following expression:

$$G(V) = (\pi r^2/l)\gamma\omega_p z e_0 C_0 \times \frac{\phi(A)-\phi(B)}{\exp(z e_0\phi(A)/kT)-\exp(z e_0\phi(B)/kT)} \times \frac{1-\exp(z e_0 V/kT)}{V} \quad \text{(B1)}$$

where r, l, ω_p, z, e_0, C_0, V and kT have the same

meaning as in Eqn. A2. γ is a partition coefficient between bulk solution and pore interior; $\phi(A)$ and $\phi(B)$ are the potentials at the two mouthes of the channel.

Eqn. B1 cannot be directly used because $\phi(A)$ and $\phi(B)$ are given only in implicit form [25]. However, if we make the strong approximation that all the applied voltage drops linearly inside the channel we may write:

$$\phi(A) = \psi(A) \tag{B2}$$

$$\phi(B) = \psi(B) + V \tag{B3}$$

where $\psi(A)$ and $\psi(B)$ are the potentials generated at the mouthes A and B by the fixed charges. Making use of Eqns. B2 and B3 Eqn. B1 becomes:

$$G(V) = (\pi r^2/l)\gamma\omega_p z e_0 C_0 \times \frac{1 + [(\psi(B) - \psi(A))/V]}{\exp[z e_0(\psi(B) + V)/kT] - \exp[z e_0 \psi(A)/kT]} \times [1 - \exp(z e_0 V/kT)] \tag{B4}$$

Eqn. B4 has the required S-shape, varying between two asymptotic values that are:

$$G(\alpha) = (\pi r^2/l)\gamma\omega_p z e_o C_0 \exp(-z e_0 \psi(\alpha)/kT) \tag{B5}$$

where α is A or B, which correspond to large negative and large positive applied potentials, respectivel. Putting $\gamma = 1$ Eqn. B5 is equal to Eqn. A2 and so we may apply the rest of calculations of Appendix A to this case as well. In particular the Nelson procedure can be used to evaluate the potentials $\psi(A)$ and $\psi(B)$.

Acknowledgements

We wish to thank Dr. A. Gliozzi for helpful discussions and criticism and Dr. B.W. Noble for commenting on the manuscript. We are also indebted to Mr. G. Chini and Mrs. E. Agostini for excellent technical assistance. This work was supported in part by the National Research Council.

References

1 Van Bruggen, E.F.J., Wiebenga, E.M. and Gruber, M. (1962) J. Mol. Biol. 4, 1–7
2 Pant, M.C. and Conran, P. (1972) J. Membrane Biol. 8, 357–362
3 Menestrina, G. and Antolini, R. (1979) Biochem. Biophys. Res. Commun. 88, 433–439
4 Antolini, R. and Menestrina, G. (1981) Biochim. Biophys. Acta 649, 121–124
5 Latorre, R., Alvarez, O., Ehrenstein, G., Espinoza, M. and Ryes, J. (1975) J. Membrane Biol. 25, 163–182
6 Menestrina, G. and Antolini, R. (1981) Biochim. Biophys. Acta 643, 616–625
7 Menestrina, G. and Antolini, R. (1981) Period. Biol. 83, 166–170
8 McIntosh, T.J., Robertson, J.D., Ting-Beall, H.P., Walter, A. and Zampighi, G. (1980) Biochim. Biophys. Acta 601, 289–301
9 Szabo, G., Eisenman, G. and Ciani, S. (1969) J. Membrane Biol. 1, 346–352
10 Antolini, R. and Menestrina, G. (1979) Gazz. Chim. Ital. 109, 449–452
11 Blumenthal, R. (1975) Ann. N.Y. Acad. Sci. 64, 479–482
12 Alvarez, O., Diaz, E. and Latorre, R. (1975) Biochim. Biophys. Acta 389, 444–448
13 Ehrenstein, G. and Lecar, H. (1977) Q. Rev. Biophys. 10, 1–34
14 Alvarez, O., Latorre, R. and Verdugo, P. (1975) J. Gen. Physiol. 65, 421–439
15 Edmonds, D.T. (1980) Proc. R. Soc. Lond. B 211, 51–62
16 Klarman, A., Shaklai, N. and Daniel, E. (1972) Biochim. Biophys. Acta 257, 150–157
17 Veath, W.R. and Stryer, L. (1977) J. Mol. Biol. 113, 89–102
18 Apell, H.J., Bamberg, E., Alpes, M. and Läuger, P. (1977) J. Membrane Biol. 31, 171–188
19 Maniacco, D. (1981) Tesi di Laurea, Libera Università degli Studi di Trento
20 Latorre, R. and Alvarez, O. (1981) Physiol. Rev. 61, 77–150
21 Antolini, R. and Menestrina, G. (1979) FEBS Lett. 100, 377–381
22 Alvarez, O., Reyes, J. and Latorre, R. (1977) Biophys. J. 17, 214a
23 Nelson, A.P. and McQuarrie, O.A. (1975) J. Theor. Biol. 55, 13–27
24 Brown, R.H., Jr. (1974) Progr. Biophys. Mol. Biol. 28, 341–370
25 Läuger, P. and Neumke, B. (1973) in Membranes (Eisenmann, G., ed.) Vol. 2, pp. 1–59, Marcel Dekker, New York
26 Cecchi, X., Alvarez, O. and Latorre, R. (1981) J. Gen. Physiol. 78, 657–681